

Large-Scale Simulations of the Two-Dimensional Melting of Hard Disks

C. H. Mak

*Department of Chemistry, University of Southern California,
Los Angeles, California 90089-0482, USA*

(Dated: November 7, 2018)

Large-scale computer simulations involving more than a million particles have been performed to study the melting transition in a two-dimensional hard disk fluid. The van der Waals loop previously observed in the pressure-density relationship of smaller simulations is shown to be an artifact of finite-size effects. Together with a detailed scaling analysis of the bond orientation order, the new results provide compelling evidence for the Halperin-Nelson-Young picture. Scaling analysis of the translational order also yields a lower bound for the melting density that is much higher than previously thought.

PACS numbers: 64.60.Fr, 64.70.Dv

A system of hard disks in two dimension (2D) is one of the simplest models of a classical fluid. But beneath the deceptive simplicity of this model, 2D hard disks exhibit a set of surprisingly rich behaviors. Unlike in three dimensions, a 2D solid possesses only quasi-long-range translational order which decays algebraically to zero at large distances [1]. Instead of the usual first-order transition in three dimensions, a 2D solid is also expected to melt into a liquid via two continuous transitions. The intervening phase called the “hexatic” was predicted by Halperin and Nelson [2, 3] and Young [4] to possess quasi-long-range bond orientation order but no long-range translational order.

Given the simplicity of the hard disk model, it would seem easy to either prove or disprove the Halperin-Nelson-Young (HNY) theory by detailed computer simulation studies. But twenty-five year after the HNY theory was first proposed, simulations that could definitively identify the nature of the melting transition are still lacking [5]. The first simulation of 2D hard disks was carried out by Alder and Wainwright [6]. Based on the appearance of a van der Waals loop in the pressure, they concluded that the melting transition must be first-order. Since then, as more computing power has become available, simulations have been carried out with increasingly larger system sizes [5, 7, 8, 9, 10, 11, 12, 13, 14, 15, 16, 17, 18, 19, 20, 21, 22, 23, 24, 25], but instead of clarifying the picture, these simulations have provided conflicting conclusions about the nature of melting transition. One consensus that did emerge from the more recent simulation studies is that the 2D hard disk system is very sensitive to finite-size effects near the melting transition. This is not unexpected if the transition is continuous, but compared to fluids with a soft potential [26] the hard disk system is much more prone to finite-size errors and boundary effects. In a simulation of up to $N = 128^2$ particles, Zollweg and Chester [9] observed that the equilibration time increased dramatically for densities very close to the melting transition – systems of this size were apparently not large enough to reach the scaling limit.

The largest simulation that has been performed to date was carried out by Jaster with up to $N = 256^2$ particles [16, 17], and more recently for two higher densities with up to $N = 1024^2$ [24]. Even though a van der Waals loop was observed in the pressure at densities between $\rho = 0.895$ and 0.910 (solid squares in Fig. 1), Jaster showed using a scaling analysis that his data were also compatible with the HNY scenario. A van der Waals loop is often the sign of a first-order transition, but it may also arise

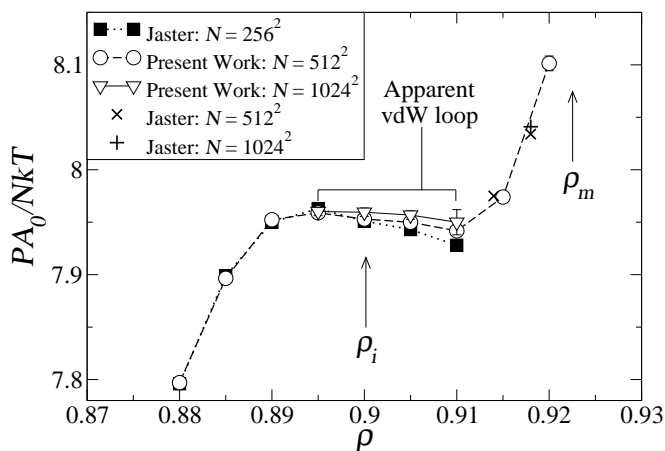


FIG. 1: Pressure of the hard disk fluid as a function of density. Solid squares are $N = 256^2$ data from Jaster [17], and crosses and plus, respectively, are $N = 512^2$ and $N = 1024^2$ data from Jaster [24]. Open circles and open squares are data from the present work for $N = 512^2$ and 1024^2 , respectively, with error bars as indicated. The dotted line is a guide to the eye through Jaster’s data for $N = 256^2$. The dashed and solid line are guides to the eye through the $N = 512^2$ and 1024^2 data in the present work. Note the presence of an apparent van der Waals (vdW) loop between $\rho = 0.895$ and 0.910 , which becomes shallower for increasingly larger size simulations. For $N = 1024^2$, the van der Waals loop between $\rho = 0.895$ and 0.905 has disappeared completely, with a small decrease in the pressure still visible for $\rho = 0.910$. The two arrows indicate the approximate locations of the isotropic-hexatic and hexatic-solid boundaries.

from finite-size errors. To definitively rule out a first-order scenario, one must demonstrate that the van der Waals loop is a finite-size artifact, i.e. it must be shown to disappear with larger size simulations. Curiously, the same van der Waals loop was observed for two different sizes in Jaster's data – the pressure for $N = 128^2$ (not shown in Fig. 1) and 256^2 coincide almost completely.

In this letter, we describe a Monte Carlo study of 2D hard disks for up to $N = 1024^2 = 1048576$ particles. The calculations were carried out in the canonical ensemble, in a square box with periodic boundary condition and in a rectangular box with aspect ratio $\sqrt{3} : 2$ for the higher densities. We worked with densities in the range $\rho = 0.880$ to 0.920 , which according to previous estimates should span the transition region [5, 6, 9, 11, 17]. Densities ρ are given in reduced units where the hard disk diameter is one.

While the rationale for going to larger system size is to eliminate finite-size effects, larger simulations also take longer to equilibrate. We have focused on $N = 512^2$ to try to carry out detailed simulations covering a large range of densities between $\rho = 0.880$ and 0.920 . At this size, one run at each density took several months of CPU time. Additional larger simulations with $N = 1024^2$ were performed for four densities between $\rho = 0.895$ and 0.910 in the vicinity of the van der Waals loop previously observed in smaller simulations. In contrast, Jaster's recent simulations [24] focuses on a different region in the phase diagram, offering data for $\rho = 0.918$ at $N = 1024^2$ and two densities, $\rho = 0.914$ and 0.918 , for $N = 512^2$.

Two different types of Monte Carlo moves were used for our simulations. The first is a conventional Metropolis move, where each particle is displaced in a random direction by a random amount. A second Monte Carlo move based on the cluster algorithm proposed by Dress and Krauth [27] and Liu and Luijten [28] was also used. At the densities we worked with, neither algorithm is particularly efficient in causing very large rearrangements in the system configuration. But by mixing two different algorithms that have vastly different properties, we hope to minimize equilibration problems characteristic of any single algorithm. One Monte Carlo step (MCS) in our simulation is defined as having moved each particle on the average once using the Metropolis algorithm, plus having made one global cluster update. The simulations reported here were carried out with no fewer than 5 million MCS for each density. Depending on the equilibration rate, results from the last 1 to 3 million MCS were used to collect statistics. Two to four independent simulations were carried out for each density for simulations with a square box, and five to six for those with a rectangular box.

The pressure P was calculated using the virial formula $PA_0/NkT = [1 + \pi\rho g(1^+)/2]\sqrt{3}\rho/2$, where $g(1^+)$ is the contact value of the pair correlation function and $A_0 = \sqrt{3}N/2$ is the closed-packed area of the system.

The calculated pressure P is shown in Fig. 1 as a function of density ρ for $N = 512^2$ (open circles) and for $N = 1024^2$ (open triangles). Comparing the $N = 512^2$ and 1024^2 data to those from Jaster's simulation with $N = 256^2$, the two sets of data are almost identical for $\rho \leq 0.890$, but inside the range $\rho = 0.895$ to 0.910 , the larger size simulations produced a smaller pressure for $\rho = 0.895$ but larger pressures for $\rho = 0.900$ to 0.910 . It is therefore clear that the apparent van der Waals loop in the pressure is a result of finite-size effects, and using even larger size simulations, this slight nonmonotonic decrease in the pressure should eventually vanish altogether. For the $N = 1024^2$ simulations, the van der Waals loops has completely disappeared between $\rho = 0.895$ and 0.905 , with a slight dip in P still visible for $\rho = 0.910$. As expected, finite-size effects are indeed very pronounced in the transition region even for simulations of this magnitude.

Even though the evidence in Fig. 1 is compelling that the van der Waals loop is an artifact of finite-size effects, these data alone cannot definitively rule out a first-order melting transition. For this, we need to carefully analyze the finite size effects. To disentangle the finite-size effects, a detailed scaling analysis must be performed on the simulation data. We have found a subblock scaling analysis [11, 26] to be useful for this purpose. With this method, a single large size simulation provides information on multiple length scales simultaneously. The subblock scaling analysis was applied to the bond orientation order as well as the translational order.

The bond orientation order is given by $\psi_6^2 = |(6N)^{-1} \sum_l \sum_j \exp(6i\theta_{lj})|^2$, where the sum goes over each particles l and its nearest neighbors j and θ_{lj} is the angle between the line from l to j with some fixed reference axis. According to HNY theory, ψ_6 should have only short-range order in the isotropic phase and quasi-long-range order in the hexatic phase with exponent $\eta_6 \leq 1/4$. We calculated ψ_6 for subblock sizes of $L_B = L/64, L/32 \dots L$, where L is the full length of the box and plot the results in Fig. 2. For $\rho \leq 0.895$, ψ_6 clearly scales to zero, but for $\rho \geq 0.900$, ψ_6 appears to scale to a finite value.

To establish the precise scaling behavior, we plot $\ln \psi_6^2$ vs. the natural log of the length of the subblock L_B in Fig. 3 for the $N = 512^2$ simulations. According to HNY theory, this plot should show a slope $-\eta_6$ in the hexatic phase and -2 in the isotropic phase where there is only short-range order. Figure 3 shows that for both $\rho = 0.880$ (solid triangles) and 0.890 (open diamonds), the bond orientation order has no long-ranged correlations in the long length scale limit, and the size of the simulations was large enough to reach the scaling limit. We can safely conclude that densities $\rho \leq 0.890$ are in the isotropic phase. On the other hand, for the highest densities $\rho = 0.905$ (solid diamonds) and 0.910 (open squares), the bond orientation order shows an algebraic decay with an exponent η_6 much smaller than $1/4$. This

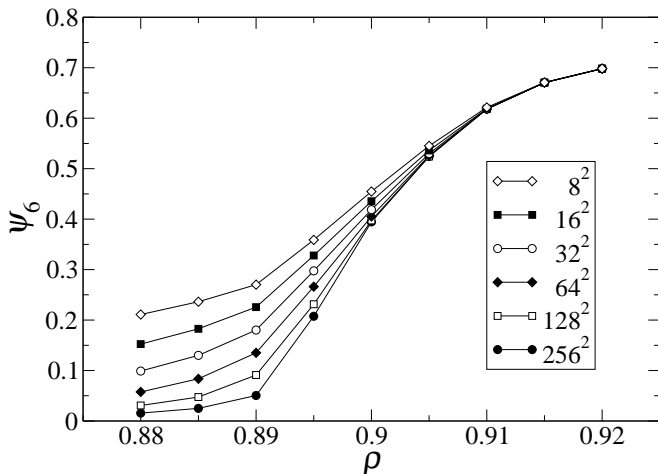


FIG. 2: The bond orientation order parameter ψ_6 derived from the subblock analysis as a function of density for the $N = 512^2$ simulations. For $\rho \leq 0.895$, ψ_6 scales to 0 with larger system sizes. For $\rho \geq 0.905$, ψ_6 appears to scale to a nonzero value.

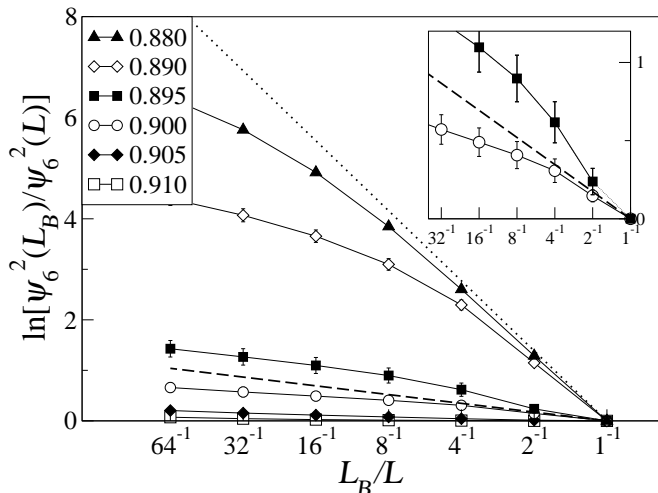


FIG. 3: Subblock scaling analysis for the bond orientation order parameter for the $N = 512^2$ simulations. The dotted line corresponds to a slope of -2 and the dashed line a slope of $-1/4$. The inset shows an expanded view for $\rho = 0.895$, 0.900 and 0.905 in the large length scale region.

is consistent with the interpretation that these densities are either inside the hexatic or the solid phase.

For the two densities $\rho = 0.895$ and 0.900 , the interpretation of the subblock scaling plots is more involved. The inset in Fig. 3 shows an expanded view of their behaviors in the large length scale limit. For $\rho = 0.900$ (open circles), the bond orientation order shows a slope that is very close to $-1/4$ at large length scales. In the HNY scenario, this is consistent with a density inside the hexatic phase, very close to the hexatic-isotropic boundary ρ_i . These evidence suggest that $\rho_i \lesssim 0.900$.

For $\rho = 0.895$ (closed squares), the subblock scaling

plot changes slope twice, first at $L/2$ and then more gradually between $L/4$ and $L/8$. The first abrupt slope change at $L/2$ is an artifact of the subblock scaling analysis which has been discussed by Weber, Marx and Binder [11]. The reason for this sudden slope change is that the subblocks and the full box actually belongs to two different ensembles – the canonical for the full box and something resembling the grand canonical for the subblocks. It is therefore possible for the full box to exhibit a different scaling behavior compared to the subblocks when the correlation length exceeds the size of the simulation box, in which case the full box data point must be excluded from the scaling analysis. When this is done, the scaling behavior suggests that the orientation order decays algebraically with an exponent larger than $1/4$. But clearly the scaling limit has not been reached, so it is possible that this exponent will continue to increase with lengths beyond the size of the present simulation. These evidence suggest that $\rho = 0.895$ must still be inside the isotropic phase but is very close to the isotropic-hexatic boundary.

Taken together, the pressure data and the subblock scaling analysis of the bond orientation order reveal a consistent picture. For densities $\rho \leq 0.895$, the system is in the isotropic phase. The van der Waals loop in the pressure between $\rho = 0.895$ and 0.910 observed in previous simulations is most certainly due to finite-size effects. The bond orientation correlation length increases when the isotropic-hexatic boundary ρ_i is approached from below and it changes from short-range correlation to an algebraic decay with η_6 close to $1/4$ at $\rho_i \lesssim 0.900$, which is consistent with previous estimates [17]. Above ρ_i , the exponent η_6 decreases quickly from $1/4$ to zero when the hexatic-solid boundary ρ_m is approached from below. These findings are consistent with the HNY scenario.

The fact that $\eta_6 \rightarrow 0$ for $\rho \rightarrow 0.910$ has been used previously to suggest that the hexatic-solid boundary is at $\rho_m \approx 0.910$ [11, 17]. The recent data of Jaster, however, have placed ρ_m at a much higher value ≈ 0.933 [24]. To more accurately locate the hexatic-solid boundary ρ_m , we turn to a subblock scaling analysis of the translational order $\psi_t^2 = |N^{-1} \sum_l \exp(i\vec{k} \cdot \vec{r}_l)|^2$, where the wavevector \vec{k} has magnitude $2\pi/(\sqrt{3}/2\rho)^{1/2}$. In the solid phase, ψ_t^2 is expected to decay algebraically with exponent $\eta_t = 1/3$. The results for three densities, $\rho = 0.900$, 0.910 and 0.920 , are shown in Fig. 4 for the $N = 512^2$ simulations in both a square and a rectangular box with a $\sqrt{3} : 2$ aspect ratio. For $\rho = 0.900$ (triangles) and 0.910 (squares), the results are consistent with no long-range translational order in the large length scale limit for both box geometries. This indicates that both of these densities are inside the hexatic phase. On the other hand, for $\rho = 0.920$, the translational order shows apparently different scaling behaviors for the two box geometries – no long-range order in the square box but quasi-long-range translational order with an apparent exponent $\eta_t > 1/3$ for the rectangular box. In fact, comparing the two dif-

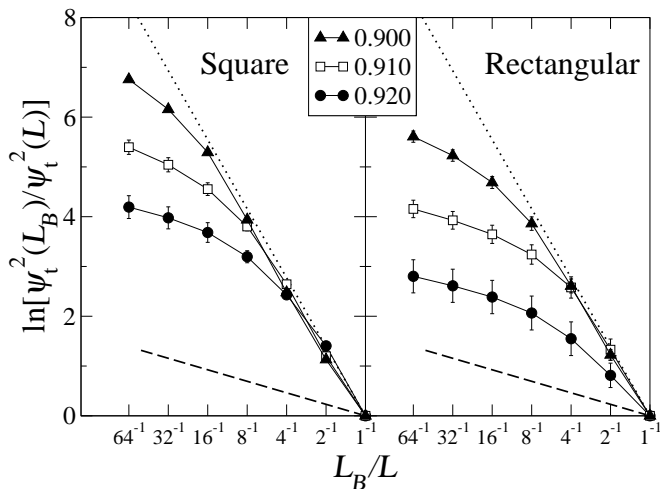


FIG. 4: Subblock scaling analysis for the translational order parameter for the $N = 512^2$ simulations in a square box and a rectangular box. The dotted line corresponds to a slope of -2 and the dashed line a slope of $-1/3$.

ferent box geometries, we found that the rectangular box simulations at this density were much slower to equilibrate, leading to the larger error bars on the right panel of Fig. 4 for $\rho = 0.920$. Since the translational correlation length is expected to diverge according to HNY theory as ρ approaches the melting density ρ_m [3], the rectangular box used for the simulations at $\rho = 0.920$ was probably too small to reach the scaling limit. Therefore, we believe that $\rho = 0.920$ is most likely still inside the hexatic phase and has not yet reached the hexatic-solid boundary. This establishes a lower bound for ρ_m , one that is much higher than the value previously suggested [11, 17]. But this new lower bound is consistent with the recent estimate provided by Jaster based on simulations with N up to 1024^2 [24]. Since the pressure at $\rho = 0.920$ (see Fig. 1) is much higher than the pressure inside the apparent van der Waals loop, this new lower bound for ρ_m also provides evidence corroborating the conclusion we have drawn from the size-dependence of the pressure-density data in Fig. 1 that the apparent van der Waals loop in the pressure is not related to a first-order transition.

In conclusion, we have shown using large-scale computer simulations with more than a million particles that the apparent van der Waals loop observed previously in smaller simulations is an artifact of finite-size effects. In conjunction with a detailed scaling analysis, the data provide compelling evidence for a continuous isotropic-hexatic transition as predicted by HNY theory at $\rho_i \lesssim 0.900$. Scaling analysis of the translational order also yields a lower bound for the melting density, $\rho_m > 0.920$, one that is much higher than previously thought, providing additional evidence that the apparent

van der Waals loop is not due to a first-order transition.

This work was supported by the National Science Foundation under grant CHE-9970766. The author has benefited from helpful discussions with Hans C. Andersen.

-
- [1] N.D. Mermin and H. Wagner, *Phys. Rev. Lett.* **17**, 1133 (1966).
 - [2] B.I. Halperin and D.R. Nelson, *Phys. Rev. Lett.* **41**, 121 (1978).
 - [3] D.R. Nelson and B.I. Halperin, *Phys. Rev. B* **19**, 2457 (1979).
 - [4] A.P. Young, *Phys. Rev. B* **19**, 1855 (1979).
 - [5] K. Binder, S. Sengupta and P. Nielaba, *J. Phys. Condens. Matt.* **14**, 2323 (2002).
 - [6] B.J. Alder and T.E. Wainwright, *Phys. Rev.* **127**, 359 (1962).
 - [7] W.G. Hoover and F.H. Ree, *J. Chem. Phys.* **49**, 3609 (1968).
 - [8] J.A. Zollweg, G.V. Chester and P.W. Leung, *Phys. Rev. B* **39**, 9518 (1989).
 - [9] J.A. Zollweg and G.V. Chester, *Phys. Rev. B* **46**, 11187 (1992).
 - [10] J. Lee and K.J. Strandburg, *Phys. Rev. B* **46**, 11190 (1992).
 - [11] H. Weber, D. Marx and K. Binder, *Phys. Rev. B* **51**, 14636 (1995).
 - [12] A.C. Mitus, H. Weber and D. Marx, *Phys. Rev. E* **55**, 6855 (1997).
 - [13] J.F. Fernandez, J.J. Alonso and J. Stankiewicz, *Phys. Rev. Lett.* **75**, 3477 (1995).
 - [14] J.F. Fernandez, J.J. Alonso and J. Stankiewicz, *Phys. Rev. E* **55**, 750 (1997).
 - [15] A. Jaster, *Europhys. Lett.* **42**, 277 (1998).
 - [16] A. Jaster, *Physica A* **264**, 134 (1999).
 - [17] A. Jaster, *Phys. Rev. E* **59**, 2594 (1999).
 - [18] M.A. Bates and D. Frenkel, *Phys. Rev. E* **61**, 5223 (2000).
 - [19] S. Sengupta, P. Nielabe and K. Binder, *Phys. Rev. E* **61**, 6294 (2000).
 - [20] A.C. Mitus, A.Z. Patashinski, A. Patrykiewicz and S. Sokolowski, *Phys. Rev. B* **66**, 184202 (2002).
 - [21] H. Watanabe, S. Yukawa, Y. Ozeki and N. Ito, *Phys. Rev. E* **66**, 041110 (2002).
 - [22] K.W. Wojciechowski, K.V. Tretyakov, A.C. Branka and M. Kowalik, *J. Chem. Phys.* **119**, 939 (2003).
 - [23] Binder K, Chaudhuri D, Franzrahe K, Henseler P, Lohrer M, Ricci A, Sengupta S, Strepp W Nielaba P, *J. Phys. Cond. Matt.* **16**, S4115 (2004).
 - [24] A. Jaster, *Phys. Lett. A* **330**, 120 (2004).
 - [25] H. Watanabe, S. Yukawa, Y. Ozeki and N. Ito, *Phys. Rev. E* **69**, 045103 (2004).
 - [26] K. Bagchi, H.C. Andersen and W. Swope, *Phys. Rev. Lett.* **76**, 255 (1996).
 - [27] C. Dress and W. Krauth, *J. Phys. A* **28**, L597 (1995).
 - [28] J.W. Liu and E. Luijten, *Phys. Rev. Lett.* **92**, 035504 (2004).